9-2006

# Synthesis, Structure, Anion Binding, And Sensing By Calix[4] Pyrrole Isomers

Ryuhei Nishiyabu

Manuel A. Palacios

Wim Dehaen

Pavel Anzenbacher Jr.
*Bowling Green State University*, pavel@bgsu.edu

J|A|C|S
ARTICLES
Published on Web 08/16/2006

# Synthesis, Structure, Anion Binding, and Sensing by Calix[4]pyrrole Isomers

Ryuhei Nishiyabu,[†] Manuel A. Palacios,[†] Wim Dehaen,[‡] and Pavel Anzenbacher, Jr.*,[†]

*Contribution from the Department of Chemistry and Center for Photochemical Sciences, Bowling Green State University, Bowling Green, Ohio 43403, and Department of Chemistry, Katholieke Universiteit Leuven, Celestijnenlaan 200F, 3001 Leuven, Belgium*

Received April 14, 2006; E-mail: pavel@bgnet.bgsu.edu

***Abstract:*** The synthesis, structure, and anion binding properties of chromogenic octamethylcalix[4]pyrroles (OMCPs) and their N-confused octamethylcalix[4]pyrrole isomers (NC-OMCPs) containing an inverted pyrrole ring connected via $\alpha'$- and $\beta$-positions are described. X-ray diffraction analyses proved the structures of two synthesized isomeric pairs of OMCPs and NC-OMCPs. The addition of anions to solutions of chromogenic OMCPs and NC-OMCPs resulted in different colors suggesting different anion-binding behaviors. The chromogenic NC-OMCPs showed significantly stronger anion-induced color changes compared to the corresponding chromogenic OMCP, and the absorption spectroscopy titrations indicated that chromogenic OMCPs and NC-OMCPs also possess different anion binding selectivity. Detailed NMR studies revealed that this rather unusual feature stems from a different anion-binding mode in OMCPs and NC-OMCPs, one where the $\beta$-pyrrole C−H of the inverted pyrrole moiety participates in the hydrogen-bonded anion−NC-OMCP complex. Preliminary colorimetric microassays using synthesized chromogenic calixpyrroles embedded in partially hydrophilic polyurethane matrices allow for observation of analyte-specific changes in color when the anions are administered in the form of their aqueous solutions and in the presence of weakly competing anions.

## Introduction

Octamethylcalix[4]pyrrole (OMCP, **1**), a tetrapyrrole macrocycle first prepared by Baeyer,[1] garnered significant attention recently due to its ability to bind small anions[2] and electroneutral molecules.[3] After the discovery of its supramolecular properties,[1−8] OMCP has become the subject of numerous efforts devoted to understanding, improving, and tuning the binding affinity and selectivity toward anions by preparation of substituted OMCP[9−18] and further related compounds such as expanded calix[*n*]pyrroles,[19−27] calixbipyrrole,[28−32] strapped calixpyrrole,[33−37] calixpyrrole dimer,[38] and cryptand-like calixpyrrole.[39] Furthermore,

[†] Bowling Green State University.
[‡] Katholieke Universiteit Leuven.

(1) Baeyer, A. *Ber. Dtsch. Chem. Ges.* **1886**, *19*, 2184−2185.
(2) Gale, P. A.; Sessler, J. L.; Král, V.; Lynch, V. *J. Am. Chem. Soc.* **1996**, *118*, 5140−5141.
(3) Allen, W. E.; Gale, P. A.; Brown, C. T.; Lynch, V. M.; Sessler, J. L. *J. Am. Chem. Soc.* **1996**, *118*, 8, 12471−12472.
(4) Custelcean, R.; Delmau, L. H.; Moyer, B. A.; Sessler, J. L.; Cho, W.-S.; Gross, D.; Bates, G. W.; Brooks, S. J.; Light, M. E.; Gale, P. A. *Angew. Chem., Int. Ed.* **2005**, *44*, 2537−2542.
(5) Nielsen, K. A.; Cho, W.-S.; Jeppesen, J. O.; Lynch, V. M.; Becher, J.; Sessler, J. L. *J. Am. Chem. Soc.* **2004**, *126*, 16296−16297.
(6) Gale, P. A.; Sessler, J. L.; Král, V. *Chem. Commun.* **1998**, 1−8.
(7) Gale, P. A.; Anzenbacher, P., Jr.; Sessler, J. L. *Coord. Chem. Rev.* **2001**, *222*, 57−102.
(8) Sessler, J. L.; Andrievsky, A.; Gale, P. A.; Lynch, V. *Angew. Chem., Int. Ed. Engl.* **1996**, *35*, 2782−2785.
(9) Miyaji, H.; An, D.; Sessler, J. L. *Supramol. Chem.* **2001**, *13*, 661−669.
(10) Anzenbacher, P., Jr.; Try, A. C.; Miyaji, H.; Jursíková, K.; Lynch, V. M.; Marquez, M.; Sessler, J. L. *J. Am. Chem. Soc.* **2000**, *122*, 10268−10272.
(11) Anzenbacher, P., Jr.; Jursíková, K.; Shriver, J. A.; Miyaji, H.; Lynch, V. M.; Sessler, J. L.; Gale, P. A. *J. Org. Chem.* **2000**, *65*, 7641−7645.
(12) Gale, P. A.; Sessler, J. L.; Allen, W. E.; Tvermoes, N. A.; Lynch, V. *Chem. Commun.* **1997**, 665−666.
(13) Warriner, C. N.; Gale, P. A.; Light, M. E.; Hursthouse, M. B. *Chem. Commun.* **2003**, 1810−1811.
(14) Woods, C. J.; Camiolo, S.; Light, M. E.; Coles, S. J.; Hursthouse, M. B.; King, M. A.; Gale, P. A.; Essex, J. W. *J. Am. Chem. Soc.* **2002**, *124*, 8644−8652.
(15) Camiolo, S.; Gale, P. A. *Chem. Commun.* **2000**, 1129−1130.
(16) Anzenbacher, P., Jr.; Jursíková, K.; Lynch, V. M.; Gale, P. A.; Sessler, J. L. *J. Am. Chem. Soc.* **1999**, *121*, 11020−11021.
(17) Bonomo, L.; Solari, E.; Toraman, G.; Scopelliti, R.; Latronico, M.; Floriani, C. *Chem. Commun.* **1999**, 2413−2414.
(18) Gale, P. A.; Sessler, J. L.; Lynch, V.; Sansom, P. I. *Tetrahedron Lett.* **1996**, *37*, 7881−7884.
(19) Sessler, J. L.; Cho, W.-S.; Gross, D. E.; Shriver, J. A.; Lynch, V. M.; Marquez, M. *J. Org. Chem.* **2005**, *70*, 5982−5986.
(20) Piatek, P.; Lynch, V. M.; Sessler, J. L. *J. Am. Chem. Soc.* **2004**, *126*, 16073−16076.
(21) Cafeo, G.; Kohnke, F. H.; Parisi, M. F.; Nascone, R. P.; La Torre, G. L.; Williams, D. J. *Org. Lett.* **2002**, *4*, 2695−2697.
(22) Sessler, J. L.; Anzenbacher, P., Jr.; Shriver, J. A.; Jursíková, K.; Lynch, V. M.; Marquez, M. *J. Am. Chem. Soc.* **2000**, *122*, 12061−12062.
(23) Arumugam, N.; Jang, Y.-S.; Lee, C.-H. *Org. Lett.* **2000**, *2*, 3115−3117.
(24) Cafeo, G.; Kohnke, F. H.; La Torre, G. L.; White, A. J. P.; Williams, D. J. *Angew. Chem., Int. Ed.* **2000**, *39*, 1496−1498.
(25) Cafeo, G.; Kohnke, F. H.; La Torre, G. L.; White, A. J. P.; Williams, D. J. *Chem. Commun.* **2000**, 1207−1208.
(26) Turner, B.; Botoshansky, M.; Eichen, Y. *Angew. Chem., Int. Ed.* **1998**, *37*, 2475−2478.
(27) Gale, P. A.; Genge, J. W.; Král, V.; McKervey, M. A.; Sessler, J. L.; Walker, A. *Tetrahedron Lett.* **1997**, *38*, 8443−8444.
(28) Sessler, J. L.; An, D.; Cho, W.-S.; Lynch, V. M.; Yoon, D.-W.; Hong, S.-J.; Lee, C.-H. *J. Org. Chem.* **2005**, *70*, 1511−1517.
(29) Sessler, J. L.; An, D.; Cho, W.-S.; Lynch, V.; Marquez, M. *Chem.−Eur. J.* **2005**, *11*, 2001−2011.
(30) Sessler, J. L.; An, D.; Cho, W.-S.; Lynch, V.; Marquez, M. *Chem. Commun.* **2005**, 540−542.
(31) Sessler, J. L.; An, D.; Cho, W.-S.; Lynch, V. *J. Am. Chem. Soc.* **2003**, *125*, 13646−13647.
(32) Sessler, J. L.; An, D.; Cho, W.-S.; Lynch, V. *Angew. Chem., Int. Ed.* **2003**, *42*, 2278−2281.


**10.1021/ja0622150 CCC: $33.50** 

OMCP has been applied in fabrication of HPLC supports for anion separation,[40] ion extractant,[41] and, most notably, optical[42−46] and electrochemical[47−51] anion sensors. This is mainly because calix[4]pyrroles, despite binding anions via hydrogen bonds, show unique affinity for biologically important anions such as chloride and phosphate, even in the presence of competing media such as water and electrolytes.[42] Recently, N-confused calix[4]pyrrole (NC-OMCP, **2**), an isomer containing an inverted pyrrole ring connected via α′- and β-positions, was also reported by Dehaen.[52]

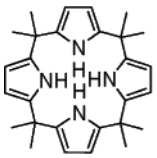

**1**

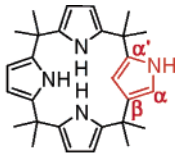

**2**

Our recent work on electrophilic aromatic substitution of OMCP led us to investigate the reactions of OMCP with various electrophiles, including tetracyanoethene and diazonium salts to obtain chromogenic OMCP derivatives.[42,53]

In their independent studies, Dehaen and co-workers[54] also synthesized a series of azo-substituted NC-OMCPs (e.g., **Azo-2**) and demonstrated changes in color of these chromogenic NC-OMCPs in the presence of anions that indicated formation of anion−receptor complexes. We have been intrigued by the possibility to synthesize pairs of regular and N-confused calix[4]pyrrole receptors and sensors and compare their anion-binding behaviors because we believed that both OMCPs and their corresponding NC-OMCPs could show unique features stemming from a different structure and different p$K_a$ of hydrogen-bond donors.[55,56]

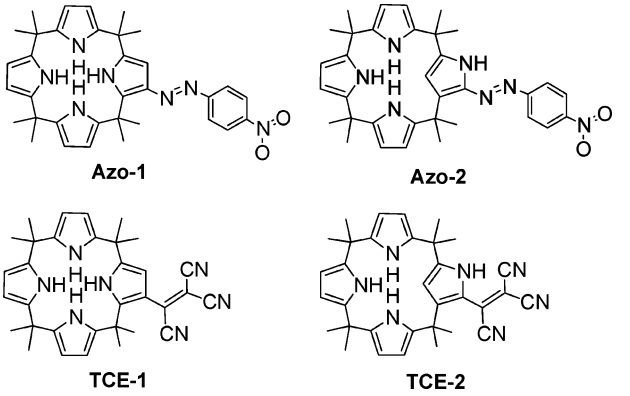


***Figure 1.*** Structures of **Azo-1**, **Azo-2**, **TCE-1**, and **TCE-2**.

***Scheme 1***

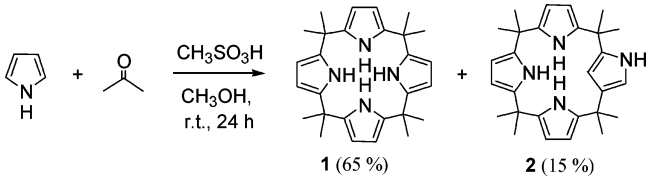


Here we report on syntheses, structures, and anion-binding properties of chromogenic NC-OMCPs together with corresponding OMCPs. Previously we have synthesized chromogenic OMCPs such as **TCE-1**[42] and **Azo-1**[57] by electrophilic substitution reaction and studied their anion binding properties. Particularly **TCE-1** demonstrated its strong anion binding affinity and selectivity as well as ability to act as colorimetric sensors for anions.[42] For this study, we have developed a new high-yielding synthesis of NC-OMCP, adopted the above modifications for the preparation of NC-OMCP-based congeners, and compared anion-binding properties of the chromogenic OMCP and NC-OMCP as well as the parent OMCP and NC-OMCP. The structures of the isomer pairs **Azo-1**, **Azo-2**, **TCE-1**, and **TCE-2** are shown in Figure 1.

## Results and Discussion

Both the regular octamethylcalix[4]pyrrole (**1**) and N-confused octamethylcalix[4]pyrrole (**2**) were obtained from condensation of acetone and pyrrole in a MeOH/$MeSO_3H$ system in 40% and 6% yield, respectively (Scheme 1).[2,52] For the purpose of this study an adaptation of this method yielding multigram yields of the starting NC-OMCP was developed. This methodology, described in the Supporting Information, provides reliable yields of 65% and 15% for OMCP and NC-OMCP, respectively.

To obtain unambiguous evidence supporting the structural assignment of **2**, we attempted the preparation of crystals of **2** for X-ray diffraction analysis from several organic solvents, but the very similar sizes of C−H and N−H pyrrole moieties in **2** resulted mostly in highly disordered crystals as the inverted

(33) Lee, C.-H.; Lee, J.-S.; Na, H.-K.; Yoon, D.-W.; Miyaji, H.; Cho, W.-S.; Sessler, J. L. *J. Org. Chem.* **2005**, *70*, 2067−2074.
(34) Panda, P. K.; Lee, C.-H. *J. Org. Chem.* **2005**, *70*, 3148−3156.
(35) Panda, P. K.; Lee, C.-H. *Org. Lett.* **2004**, *6*, 671−674.
(36) Lee, C.-H.; Na, H.-K.; Yoon, D.-W.; Won, D.-H.; Cho, W.-S.; Lynch, V. M.; Shevchuk, S. V.; Sessler, J. L. *J. Am. Chem. Soc.* **2003**, *125*, 7301−7306.
(37) Yoon, D.-W.; Hwang, H.; Lee, C.-H. *Angew. Chem., Int. Ed.* **2002**, *41*, 1757−1759.
(38) Sato, W.; Miyaji, H.; Sessler, J. L. *Tetrahedron Lett.* **2000**, *41*, 6731−6736.
(39) Bucher, C.; Zimmerman, R. S.; Lynch, V.; Sessler, J. L. *J. Am. Chem. Soc.* **2001**, *123*, 9716−9717.
(40) Sessler, J. L.; Gale, P. A.; Genge, J. W. *Chem.−Eur. J.* **1998**, *4*, 1095−1099.
(41) Levitskaia, T. G.; Marquez, M.; Sessler, J. L.; Shriver, J. A.; Vercouter, T.; Moyer, B. A. *Chem. Commun.* **2003**, 2248−2249.
(42) Nishiyabu, R.; Anzenbacher, P., Jr. *J. Am. Chem. Soc.* **2005**, *127*, 8270−8271.
(43) Miyaji, H.; Sato, W.; Sessler, J. L. *Angew. Chem., Int. Ed.* **2000**, *39*, 1777−1780.
(44) Miyaji, H.; Sato, W.; Sessler, J. L.; Lynch, V. M. *Tetrahedron Lett.* **2000**, *41*, 1369−1373.
(45) Anzenbacher, P., Jr.; Jursíková, K.; Sessler, J. L. *J. Am. Chem. Soc.* **2000**, *122*, 9350−9351.
(46) Miyaji, H.; Anzenbacher, P., Jr.; Sessler, J. L.; Bleasdale, E. R.; Gale, P. A. *Chem. Commun.* **1999**, 1723−1724.
(47) Nielsen, K. A.; Jeppesen, J. O.; Levillain, E.; Becher, J. *Angew. Chem., Int. Ed.* **2003**, *42*, 187−191.
(48) Gale, P. A.; Bleasdale, E. R.; Chen, G. Z. *Supramol. Chem.* **2001**, *13*, 557−563.
(49) Gale, P. A.; Hursthouse, M. B.; Light, M. E.; Sessler, J. L.; Warriner, C. N.; Zimmerman, R. S. *Tetrahedron Lett.* **2001**, *42*, 6759−6762.
(50) Král, V.; Sessler, J. L.; Shishkanova, T. V.; Gale, P. A.; Volf, R. *J. Am. Chem. Soc.* **1999**, *121*, 8771−8775.
(51) Sessler, J. L.; Gebauer, A.; Gale, P. A. *Gazz. Chim. Ital.* **1997**, *127*, 723−726.
(52) Depraetere, S.; Smet, M.; Dehaen, W. *Angew. Chem., Int. Ed.* **1999**, *38*, 3359−3361.
(53) Nishiyabu, R.; Anzenbacher, P., Jr. *Abstract Book*; 13th International Symposium on Supramolecular Chemistry, Notre Dame, IN, Jul 25−30, 2004; P-3-48.
(54) Gu, R.; Depraetre, S.; Kotek, J.; Budka, J.; Wagner-Wysiecka, E.; Biernat, J. F.; Dehaen, W. *Org. Biomol. Chem.* **2005**, *3*, 2921−2923.
(55) Nechita, M. T.; Lotrean, S.; Radecki, J.; Radecka, H.; Depreatere, S.; Dehaen, W. *Pol. J. Food. Nutr. Sci.* **2003**, *12* (SI 2), 81−87.
(56) Piotrowski, T.; Radecka, H.; Radecki, J.; Depraetere, S.; Dehaen, W. *Mater. Sci. Eng., C* **2001**, *C18*, 223−228.
(57) Wex, B.; Anzenbacher, P., Jr. *Abstracts of papers*; 223rd National Meeting of the American Chemical Society, Orland, FL, Apr 7−11, 2002; American Chemical Society: Washington, DC, 2002; ORGN-245.

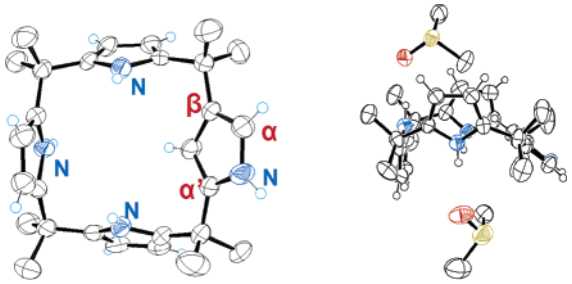

***Figure 2.*** X-ray crystal structure of **2** (thermal ellipsoids are scaled to the 30% probability level; the methyl hydrogen atoms have been removed for clarity). (Left) Structure of the receptor **2**. (Right) Inclusion of the two DMSO molecules that stabilize the conformation of the receptor in the crystal.

***Scheme 2***

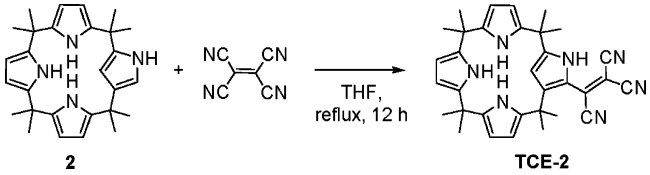

**2** **TCE-2**

pyrrole was not always found in a crystallographically unique position. This, together with the lack of stability of **2** due to a free reactive α-pyrrole moiety,[52] made it difficult to grow X-ray quality crystals. After numerous, largely unsuccessful attempts we realized that binding between **2** and a suitable hydrogen bond acceptor could lock the receptor in a bulkier and more spatially unique complex. Consequently diffraction grade crystals of **2** were grown in dimethyl sulfoxide to obtain hydrogen bonded complex **2**·2DMSO. The single-crystal X-ray analysis clearly showed the structure of **2** in which one pyrrole ring is linked through its α′- and *β*-positions instead of α- and α′-positions in **1** (Figure 2).

Tricyanoethylene substituted **1** (**TCE-1**) was prepared by electrophilic substitution of **1** with tetracyanoethylene.[42] The same reaction using **2** gave **TCE-2** (Scheme 2) where the tricyanoethylene moiety was attached at the more electron-rich α-position. This reaction yielded only one product (36% yield) as a purple solid.

Interestingly, $^1$H NMR spectrum of the obtained compound assumed to be **TCE-2** showed only three broad pyrrole NH singlet signals (8.53, 9.19, and 9.45 ppm in DMSO-$d_6$) instead of four broad pyrrole NH singlets. The disappearance of the α-pyrrole CH proton signal indicated substitution of the α-pyrrole position with the tricyanoethylene moiety, and a mass spectrum of this compound showed a molecular ion peak corresponding with that of **TCE-2**. The NMR spectra suggested that the obtained compound was not **TCE-2** but its cyclic form, resulting from intramolecular cyclization of the tricyanoethylene moiety with inverted pyrrole nitrogen (Figure 3).[58,59] Indeed, in the NMR spectrum of the obtained compound there was one sharp singlet at 11.16 ppm that could be assigned to the imine ═NH proton in **TCE-2C**.

The final confirmation of the structure assignment of **TCE-2C** came from single-crystal X-ray analysis. The crystal structure of **TCE-2C** is shown in Figure 2 with the structure of **TCE-1**.

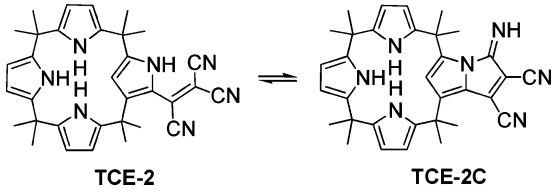

**TCE-2** **TCE-2C**

***Figure 3.*** Tautomerization of **TCE-2** to its cyclic form **TCE-2C** explains three broad $^1$H NMR resonances attributed to NH moieties and one sharp singlet attributed to the imine ═NH.

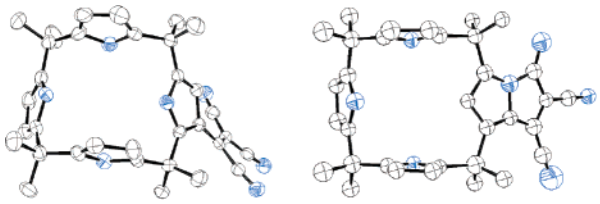

***Figure 4.*** X-ray crystal structures of **TCE-1** (left) and **TCE-2C** (right) (ORTEP, the displacement ellipsoids are scaled to the 50% probability level; the hydrogen atoms have been removed for clarity).

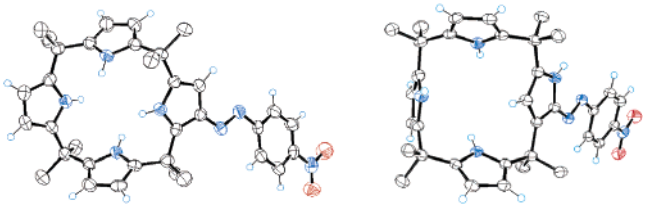

***Figure 5.*** X-ray crystal structures of **Azo-1** (left) and **Azo-2** (right) (ORTEP, the displacement ellipsoids are scaled to the 50% probability level; the methyl hydrogen atoms have been removed for clarity).

The crystal structure revealed that **TCE-2C** contains the bicyclic pyrrolizin-3-ylideneamine moiety (Figure 4).

Azo-substituted OMCP(**Azo-1**) and NC-OMCP (**Azo-2**) were also prepared by electrophilic substitution with 4-nitrobenzenediazonium tetrafluoroborate.[53,54,57] Electrophilic substitution of **2** with 4-nitrobenzenediazonium tetrafluoroborate in THF in the presence of triethylamine yielded **Azo-2** in 30% yield, while the same reaction using **1** gave a complex mixture of products including **Azo-1** in lower yield (9%). The observed lower yield of **Azo-1** could be attributed to a large number of equally reactive pyrrole *β*-positions as well as to lower reactivity of the *β*-position in **1** compared to the α-position in **2**.[60,61] The single crystals of **Azo-1** and **Azo-2** were obtained from *N*,*N*-dimethylformamide and dichloromethane/ether, respectively. The crystal structures of **Azo-1** and **Azo-2** are shown in Figure 5.

The attachment of dye precursors to **2** also converts the originally colorless species into chromogenic materials, which show changes in color upon binding of an anion. Both the naked-eye observation and the absorption spectroscopy revealed different anion binding behaviors of chromogenic OMCPs and NC-OMCPs (Figures 6 and 7).

The synthesized isomeric pairs were tested for their ability to bind anions, first by using strongly binding ($F^-$) and then by weakly binding ($Cl^-$) anions. Absorption spectra of **TCE-1** in the presence of fluoride in DMSO showed a moderate spectral change and a pink-to-orange color change, while that of chloride showed a small spectral change without a noticeable color

(58) Fares, V.; Flamini, A.; Poli, N. *J. Am. Chem. Soc.* **1995**, *117*, 11580−11581.
(59) Collange, E.; Flamini, A.; Poli, R. *J. Phys. Chem. A* **2002**, *106*, 200−208.
(60) Depraetere, S.; Dehaen, W. *Tetrahedron Lett.* **2003**, *44*, 345−347.
(61) Bulter, A. R.; Shepherd, P. T. *J. Chem. Soc., Perkin, Trans. 2* **1980**, 113−116.

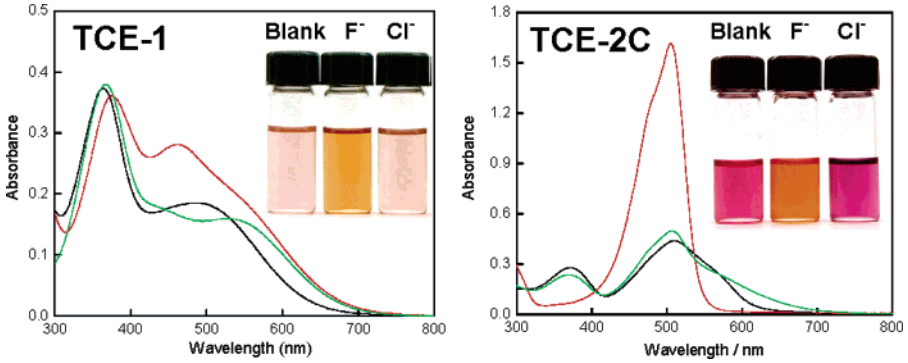


***Figure 6.*** Absorption spectra of **TCE-1** (left) and **TCE-2C** (right), both $5.0 \times 10^{-5}$ M in DMSO, in the absence of anion (black), with 10 equiv of fluoride (red), and with an excess of chloride (green). Insets: Solutions of **TCE-1** and **TCE-2C** in the absence of anion and with fluoride (10 equiv) and chloride (excess). $Bu_4N^+$ (TBA) salts of anions were used.

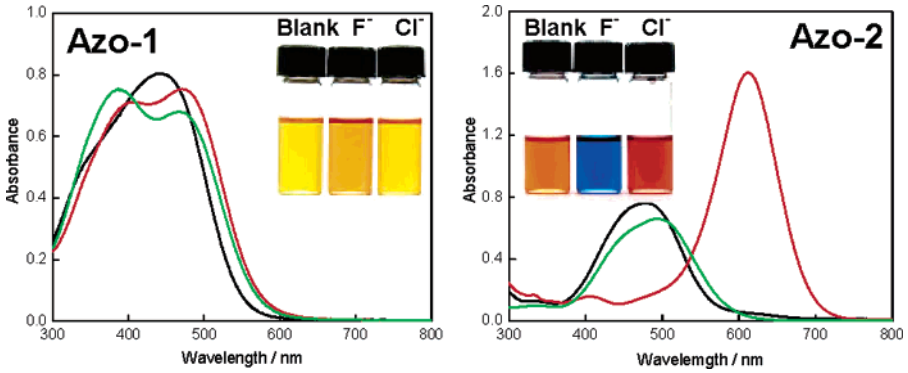


***Figure 7.*** Absorption spectra of **Azo-1** (left) and **Azo-2** (right), both $5.0 \times 10^{-5}$ M in DMSO, in the absence of anion (black), with 10 equiv of fluoride (red), and with an excess of chloride (green). Insets: Solutions of **Azo-1** and **Azo-2** in the absence of anion, with fluoride (10 equiv), and with chloride (excess). $Bu_4N^+$ (TBA) salts of anions were used.

change (Figure 6, left).[42] The solution of **TCE-2C** in DMSO showed a vivid pink color. The addition of fluoride to **TCE-2C** resulted in enhanced absorption in the 500 nm region, with a corresponding dramatic pink-to-orange color change. On the other hand, the addition of chloride into the **TCE-2C** solution resulted in a small spectral change but an easily discernible pink-to-purple color change (Figure 6, right).

Absorption spectroscopic titrations of **Azo-1** and **Azo-2** with anions were also performed. In preliminary qualitative experiments, the addition of fluoride and chloride anions into DMSO solutions of **Azo-1** resulted in the formation of two new maxima located at 385 and 467 nm and yellow-to-orange color changes (Figure 7, left). Conversely, as Dehaen reported, titrations of **Azo-2** with fluoride showed a large bathochromic shift with a dramatic orange-to-blue change in color, possibly due to the deprotonation of the inverted pyrrole NH.[54] Furthermore, **Azo-2** showed upon the addition of chloride an orange-to-red color change (Figure 7, right). The quantitative titration experiments allowed us to determine the apparent binding constants of the present chromogenic OMCPs and NC-OMCPs with anions, and the respective $K_{as}$ values are listed in Table 1.

The data in Table 1 suggest that the sensors based on the regular OMCP receptor (**TCE-1** and **Azo-1**) favor spherical anions such as fluoride and chloride. This is rationalized by the symmetry of the respective sensor−anion complex. The symmetrical conelike conformation of the OMCP receptor appears to be more suited for binding of the spherical anions. In contradistinction, sensors based on the N-confused OMCP receptor (**TCE-2/2C** and **Azo-2**) cannot adopt the almost perfectly symmetrical conelike conformation. We believe that

***Table 1.*** Association Constants for **TCE-1**, **TCE-2c**, **Azo-1**, and **Azo-2** and Anions in DMSO at 22 °C Determined by Absorption Spectroscopy Titrations[a]

| Anion | Association Constant $K_{as}$ / $M^{-1}$ | | | |
|---|---|---|---|---|
| | **TCE-1**[b] | **TCE-2C** | **Azo-1** | **Azo-2** |
| $F^-$ | $>10^6$ | $>10^6$ | $>10^6$ | 7 240 |
| $Cl^-$ | 1 370 | 319 | 741 | < 50 |
| $AcO^-$ | 242 000 | $>10^6$ | 8 540 | 16 600 |
| $H_2PO_4^-$ | 5 230 | 810 000 | 3 330 | 430 |
| $HP_2O_7^{3-}$[c] | 584 000 | n. d. | 92 200 | 5 650 |
| $K_{AcO^-}/K_{Cl^-}$ | 176 | >10 000 | 12 | 330 |
| $K_{AcO^-}/K_{H_2PO_4^-}$ | 46 | 25 | 3 | 39 |

[a] Anions were used in the form of their $Bu_4N^+$ (TBA) salts. The errors in all fits are <15%. [b] See ref 42. [c] Association constants were calculated on the assumption that pyrophosphate forms a dimer in DMSO.[62]

the twisted conelike conformation available to the N-confused OMCP receptor and the corresponding sensors is better suited for anions that can bind through more than one atom, for example, two oxygen atoms in the delocalized carboxylate anion.

Thus comparison of binding affinities for **TCE-1** and **TCE-2C** shows that both compounds strongly bind fluoride (F) and acetate (AcO) and both bind chloride (Cl) weakly. **TCE-1**, like other regular calix[4]pyrroles, does not bind dihydrogenphosphate ($H_2P$) strongly, but shows high affinity for hydrogenpyrophosphate (HPP). By comparison, **TCE-2C** that adopts a distorted conelike conformation binds dihydrogenphosphate as well as acetate with high affinity. The specific order of the binding affinities is as follows: **TCE-1**: F> HPP > AcO > $H_2P$ > Cl and **TCE-2C**: AcO > F > $H_2P$ > Cl (while the binding of pyrophosphate follows a complex pattern that cannot

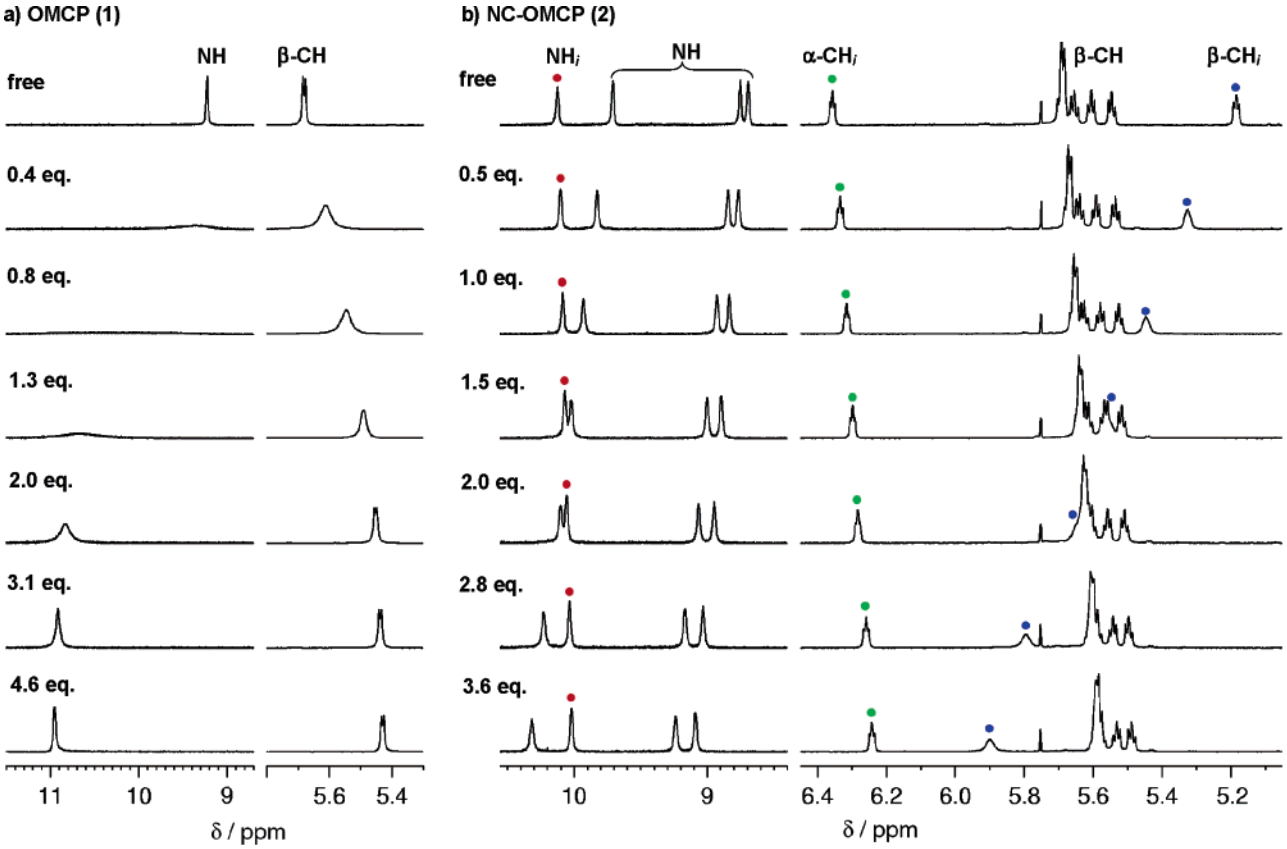


***Figure 8.*** $^1$H NMR titrations (selected regions) of $1.0 \times 10^{-2}$ M solutions of (a) **1** and (b) **2** with chloride in DMSO-$d_6$. The inverted pyrrole $^1$H resonances in **2** are labeled as follows: $NH_i$ (red), $\alpha$-$CH_i$ (green), and $\beta$-$CH_i$ (blue).

be easily numerically evaluated). Similarly, both **Azo-1** and **Azo-2** show affinity for fluoride, acetate, and hydrogenpyrophosphate, albeit weaker compared to the **TCE**-sensors. The specific order of the binding affinities is as follows: **Azo-1**: F > HPP > AcO > H2P > Cl and **Azo-2**: AcO > F > HPP > $H_2P$ > Cl.

Interestingly, both N-confused sensors (**TCE-2/2C** and **Azo-2**) show a dramatic increase in selectivity toward the acetate anion over chloride and phosphate compared to their counterparts (**TCE-1** and **Azo-1**) as evidenced by the respective selectivity coefficients expressed as ratios of binding constants $K_{AcO^-}/K_{Cl^-}$ and $K_{AcO^-}/K_{H_2PO_4^-}$. For example, the affinity for acetate over chloride increased more than 50 times for **TCE-2C** vs regular **TCE-1** and 28 times for **Azo-2** vs the regular **Azo-1**. The aspect of carboxylate-chloride selectivity is of potential practical importance, as this feature may allow sensing of carboxylate in biological milieu where the chloride and phosphate usually abound in high concentrations.

From the combination of the spectroscopic investigations and binding data expressed as relative affinity constants (Table 1), one can see that the relative strength in the respective color transitions observed for the sensors and their complexes with anions does not necessarily correlate with the receptor−anion affinities ($K_{as}$). That is most likely because the extent of the color transitions relates to the magnitude of the change in the transition dipole moment between the sensor in the resting state and in the complex. The magnitude of the change in the transition dipole moment does not generally correlate with the thermodynamic association constants but rather with the degree of difference in the frontier orbital density between the resting state and the respective receptor−anion complex. The fact that the changes in color, understood as a change in absorption wavelengths as well as a change in the absorption coefficient, which are not the same for all of the sensor−anion combinations, adds another dimension to the potential application of the reported sensors as they may be perhaps used for qualitative substrate determination in a naked-eye regime. Table 1 therefore not only shows the actual values of affinity constants but also provides a qualitative indication of the colors of the sensors and their complexes with anions.

Originally, we believed that the different affinities and selectivities between OMCP and NC-OMCP-based sensors for anions are due to the inverted-pyrrole effects on adopting a symmetrical cone conformation of the receptor, while the chromophore responsible for color change is attached to the α-position, which is closer to the pyrrole NH hydrogen bond donor then it is in the regular OMCP-based sensors where the chromophore is attached to the $\beta$-position. Later we realized that the dramatic changes in color response are unlikely to be due to a simple distance effect but most likely due to a different distribution of the frontier molecular orbitals and the corresponding $\pi-\pi^*$ transitions in the chromophores. This feature is discussed later in this paper.

Further insight into anion complexation was achieved by examination of anion binding of **1** and **2** by $^1$H NMR titrations. Titration of **1** by chloride showed a concerted downfield shift of four pyrrole NHs and an upfield shift of pyrrole $\beta$-proton signals corresponding to the formation of a symmetrical cone conformation (Figure 8a).[2,6,12,13] This is explained by the pyrrole NHs appearing close to the anion, while the $\beta$-protons face away

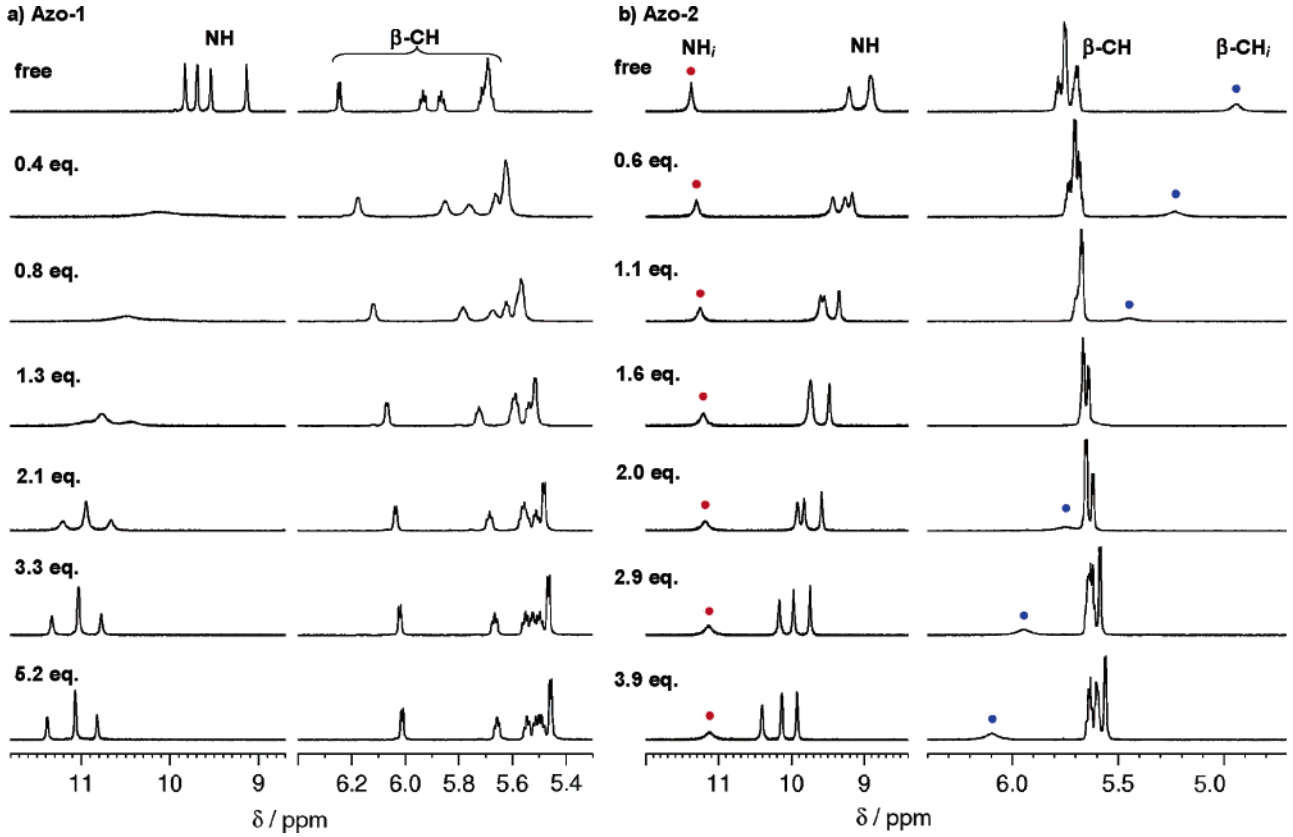


***Figure 9.*** $^1$H NMR titrations (selected regions) of $1.0 \times 10^{-2}$ M solutions of (a) **Azo-1** and (b) **Azo-2** with chloride in DMSO-$d_6$. The inverted pyrrole $^1$H resonances in **Azo-2** are labeled as follows: $NH_i$ (red) and $\beta$-$CH_i$ (blue).

from the anion and $\pi$-electrons of the other pyrroles. To our surprise, $^1$H NMR titration of **2** revealed a different pattern: the three noninverted pyrroles show the usual behavior (a downfield shift of NHs and upfield shift of the pyrrole $\beta$-H signals), while the inverted pyrrole shows a concerted upfield shift of the inverted pyrrole NH signal as well as a strong downfield shift of the $\beta$-pyrrole proton (Figure 8b).$^1$H NMR titrations of **Azo-1**, **Azo-2**, **TCE-1** (see Supporting Information), and **TCE-2C** (see Supporting Information) with chloride show the same type of behavior as **1** and **2**, respectively, suggesting the same binding behavior (Figure 9).

These results imply that the NC-OMCP receptor of **2**, **Azo-2**, and **TCE−2C** bind anions via a different binding mode compared to OMCP and OMCP-based sensors. Further insight into the binding mode was obtained from the density functional theory (DFT) study. From the combination of NMR data, and DFT energy-minimized structures, it appears that this binding mode, new in calixpyrrole-anion binding, utilizes the $\beta$-pyrrole C−H in close interaction with the anion.[49,63] Density functional theory (DFT) calculations were carried out for both OMCP and NC-OMCP and their respective complexes with tetramethylammonium fluoride (TMAF). The energy-optimized structures of complexes **1**·TMAF and **2**·TMAF are shown on computer-generated models in Figure 10.

One might think that **2** would prefer distortion of the receptor−anion complex to make all four pyrrole NHs available for hydrogen bonding. We found that the anion complexes of

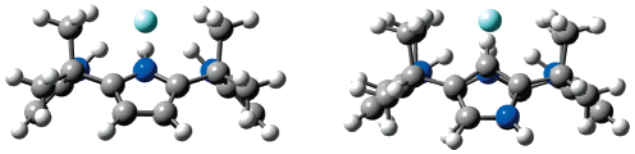

***Figure 10.*** Calculated structures of **1**·TMAF (calix[4]pyrrole·tetramethylammonium fluoride) and **2**·TMAF complexes with 1:1 binding mode. Gaussian 03[64] was used for all calculations presented. For geometry optimizations the first guesses were fully optimized by PM3 semiempirical Hamiltonian. Then, the models were reoptimized at the B3LYP/6-31G* level of theory. The $TMA^+$ is omitted here for clarity (for more details see Supporting Information).

NC-OMCPs prefer a more symmetrical, close to conelike conformation involving hydrogen-bond-like interaction to a less acidic $\beta$-pyrrole CH, rather than adopting the conformation utilizing all four pyrrole NHs. The DFT calculations also lend support to the experimental observation showing a spatial arrangement for the **2**·TMAF complex with an energy minimum for the conelike conformation. Conversely, DFT geometrical optimizations aimed at determination of an energy minimum with all four NHs participating in the fluoride anion binding failed as such conformations are too strained. The binding of basic anions such as a fluoride anion was also investigated by $^1$H NMR titration experiments of **1** and **2** combined with DFT calculations. Titration of **1** by fluoride showed a decrease in intensity of the NH proton signal of free **1**, while a new, downfield-shifted NH proton signal corresponding to the receptor−fluoride complex appeared. In these titrations coupling between those protons of **1** and the bound fluoride was observed. The respective coupling constant is 39.9 Hz.[2,6,12,13] The $^1$H NMR titration of **2** with fluoride afforded results very similar to those

(62) Chu, F.; Flatt, L. S.; Anslyn, E. V. *J. Am. Chem. Soc.* **1994**, *116*, 4194−4204.
(63) Camiolo, S.; Gale, P. A.; Hursthouse, M. B.; Light, M. E. *Org. Biomol. Chem.* **2003**, *1*, 741−744.

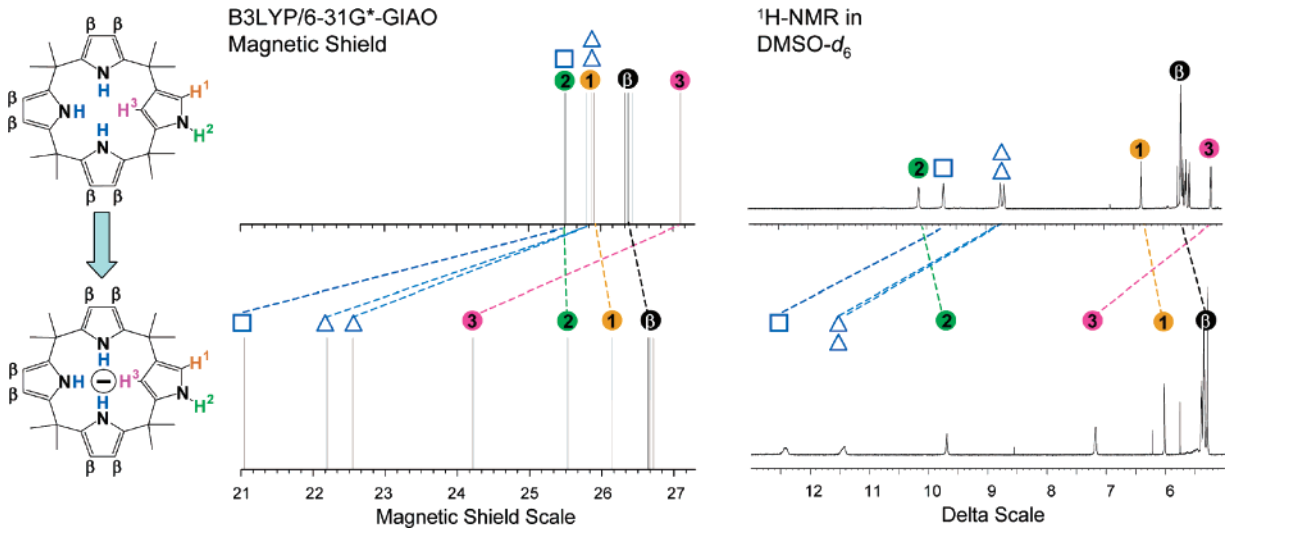


***Figure 11.*** (a) Calculated DFT-GIAO magnetic shields for NC-OMCP and NC-OMCP·TMAF in 1:1 binding mode at the B3LYP/6-31G* level of theory. (b) $^1$H NMR of **2** ($1.0 \times 10^{-2}$ M) in DMSO-$d_6$ before and after the addition of 1.85 equiv of TBAF. For details see Supporting Information.

for the $^1$H NMR titration of **2** with chloride (see Supporting Information). Here too, the concerted shifts of the three noninverted pyrrole NHs together with the $\beta$-pyrrole C−H resonance confirm the presence of a C−H−anion interaction contributing to the receptor−fluoride complex.

In the absence of the X-ray structure confirming the proposed binding mode, we performed an extensive DFT study aimed at interpretation of shifts in NMR spectra corresponding to the energy-minimized model for NC-OMCP in the resting state and in the complex with anions. Here we show the DFT-GIAO magnetic shields calculated for **2** and **2·TMAF** in the energy minimum (a conelike conformation involving the $\beta$-pyrrole hydrogen). The calculation shows the same tendency (shifts of the $^1$H-resonances) upon complexation of **2** with TMAF observed in the $^1$H NMR titration experiments for **2** with TBAF in DMSO-$d_6$ (Figure 11).

Specifically, all three NH resonances from the three regular pyrroles (ΔΔ) and the $\beta$-hydrogen of the inverted pyrrole (pink dot) shift downfield, while the $\beta$-hydrogens of the three regular pyrroles (black dot) and the NH resonance from the inverted pyrrole (green) show an upfield shift. These shifts in resonances were calculated from the structure corresponding to energy minima shown in Figure 10 and are in excellent agreement with the data recorded for N-confused calixpyrrole and its fluoride complex. We feel that these studies lend additional credibility to the binding mode anion proposed for N-confused calix[4]-pyrroles.

Interestingly, the $^1$H NMR titrations of **TCE-2C** and **Azo-2** with fluoride showed a slightly different behavior of chemical shift changes from that of **2** with fluoride. Upon the addition of fluoride to a **TCE-1** solution, four NH proton singlet signals of a free **TCE-1** disappeared and four new NH proton doublet signals appeared corresponding to the formation of a complex (Figure 12a).[42] On the other hand, titrations of **TCE-2C** with fluoride showed that the imine proton signal disappeared and three pyrrole NH signals in noninverted pyrrole rings did not show appreciable changes in chemical shifts (Figure 12b). We believe that this is due to deprotonation of the imine proton by a fluoride anion. The high acidity of the imine hydrogen is indirectly confirmed by its downfield shift (11.16 ppm in DMSO-$d_6$). While the deprotonation usually results in significant bathochromic shifts, we have observed a hypsochromic shift in absorption spectra of **TCE-2C** in the presence of 1 equiv of fluoride. We assume that this is because the deprotonation of the imine moiety results in the simultaneous opening of the pyrrolizine moiety to form **TCE-2** (Figure 3).[59]

Deprotonation of **Azo-2** by fluoride was also proposed by Dehaen, based on the similarity in shapes of absorption spectra of **Azo-2** in the presence of fluoride and hydroxide.[54] $^1$H NMR titrations of **Azo-2** with fluoride showed that the azo-substituted pyrrole NH signal as well as the three noninverted pyrrole NH signals broadened and disappeared (see Supporting Information). While the disappearance of the azo-substituted pyrrole NH and the bathochromic shift in the absorption spectrum suggest deprotonation, the disappearance of the three regular pyrrole NHs indicates rapid interconversion of multiple conformations compared to NMR time scale. The course of $^1$H NMR titration of **Azo-1** and **Azo-2** with fluoride is included in the Supporting Information.

Among the most important issues in anion sensing is the fact that anions occur mostly as solutes in water or aqueous media. While a number of anion sensors that are soluble in water-miscible solvents such as DMSO or MeCN tolerate a small percentage of water in the medium, the fact remains that most simple receptors and sensors that utilize hydrogen bonding to establish the complex do not operate successfully in water.[65]

We have previously demonstrated that some polyurethanes are capable of extracting anions from water and aqueous buffers.[42,66] Such materials doped with anion sensors utilizing hydrogen bonding to establish receptor−anion complexes may then be successfully used in conjunction with polymer matrices thereby yielding anion sensors compatible with pure water.[42,66] Based on this premise, we have developed a sensing assay using 80 ($8 \times 10$) wells ($230 \pm 10$ $\mu$m Ø, $230 \pm 10$ $\mu$m deep, Figure 13) microwell plates. Polyurethane doped with sensors were solution-cast to create ca. a 50−100 $\mu$m coating in each respective hole. Figure 13 shows a $4 \times 8$ section of the assay

(64) Frisch, M. J. et. al. *Gaussian 03*, revision B.04; Gaussian, Inc.: Pittsburgh, PA, 2003.
(65) Steed, J. W.; Atwood, J. L. *Supramolecular Chemistry*; Wiley: Chichester, 2000.
(66) Aldakov, D.; Palacios, M. A.; Anzenbacher, P., Jr. *Chem. Mater*. **2005**, *17*, 5238−5241.

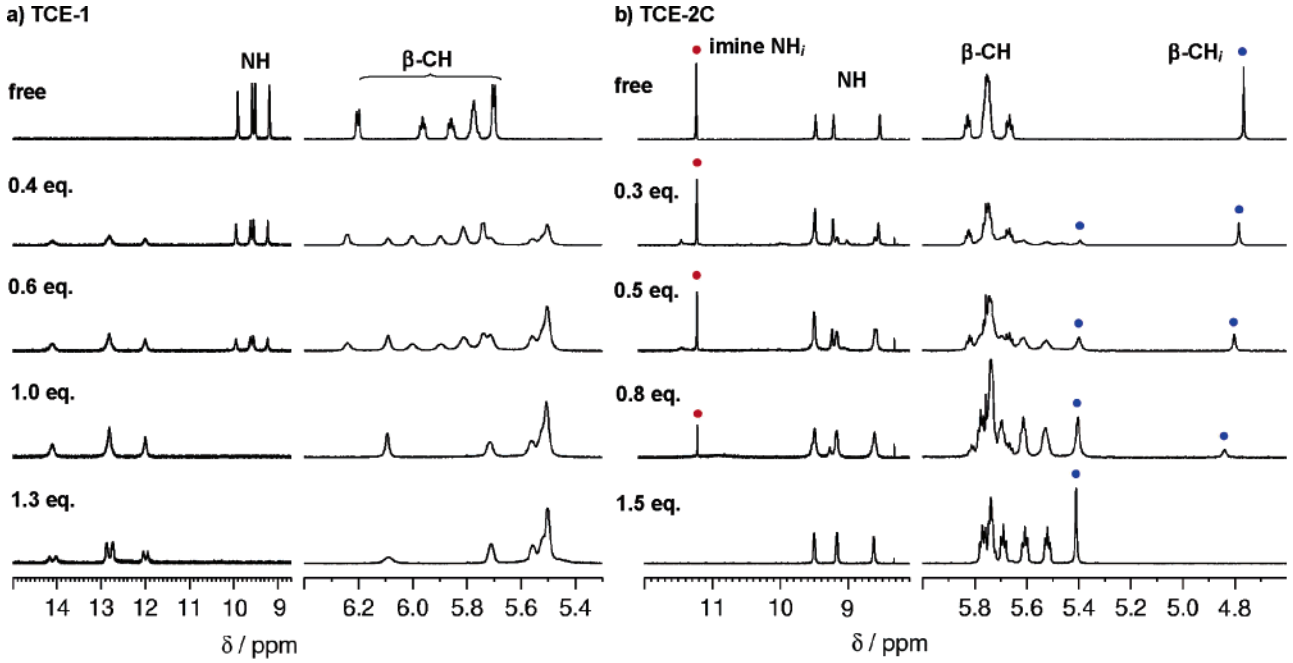


***Figure 12.*** $^1$H NMR titrations (selected regions) of $1.0 \times 10^{-2}$ M solutions of (a) **TCE-1** and (b) **TCE-2C** with fluoride in DMSO-$d_6$. The inverted pyrrole $^1$H resonances in **TCE-2C** are labeled as follows: imine $NH_i$ (red) and $\beta$-$CH_i$ (black).

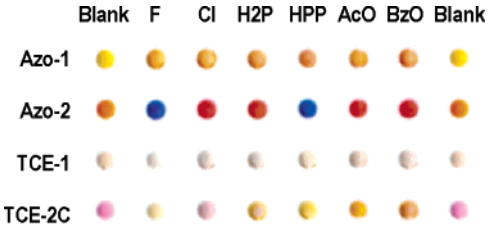


***Figure 13.*** Microassay utilizing **Azo-1**, **Azo-2**, **TCE-1**, and **TCE-2C** doped polyurethane. The respective anions were administered in pure water (200 nL, 10 mM).

that accommodates sensors **Azo-1**, **Azo-2**, **TCE-1**, and **TCE-2C** (horizontal lines) and blank (water), and six different aqueous anionic analytes (fluoride, chloride, dihydrogenphosphate, hydrogenpyrophosphate, acetate, and benzoate) in the vertical lines. The anions used in this assay were added as aqueous solutions (200 nL, 10 mM). Interestingly, changes in color observed in the DMSO−water solutions (Table 1) correspond in most cases to the color changes observed in the microassay where purely aqueous anion solutions were used. While the changes in color in the assay may be clearly observed by a naked eye, one can use a variety of absorption spectroscopy and imaging techniques to record the sensory response generated by the array. Also, the techniques of evaluating the response in the nonspecific sensor arrays[67] utilizing pattern recognition[67,68] may provide insight into an analysis of anionic analytes. The color changes in the array utilizing calixpyrrole-based sensors **Azo-1**, **Azo-2**, **TCE-1**, and **TCE-2C** suggest that these simple materials may be potentially used for sensing of anions administered as purely aqueous solutions.

While the previous microassay experiment indicated that materials **Azo-1**, **Azo-2**, **TCE-1**, and **TCE-2C** can act as

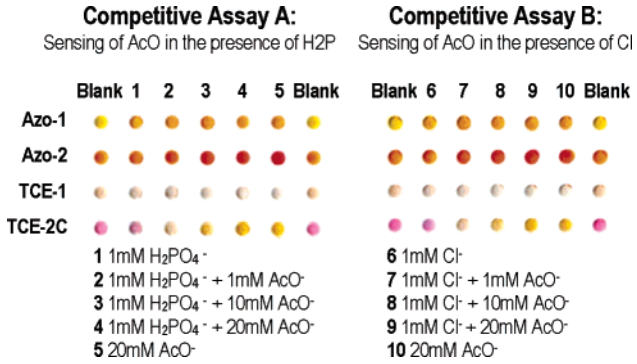


***Figure 14.*** Competitive microassay utilizing **Azo-1**, **Azo-2**, **TCE-1**, and **TCE-2C** doped polyurethane. Assay A: Sensing of acetate (0−20 mM) administered as an aqueous solution containing 1 mM $H_2PO_4^-$. Assay B: Sensing of acetate (0−20 mM) administered as an aqueous solution containing 1 mM $Cl^-$.

colorimetric sensors for aqueous anions, for practical purposes we were interested in the possibility of sensing the anions in the presence of competing electrolytes. The selectivity coefficients (see Table 1) suggest that it should be possible to sense carboxylates in the presence of chloride or phosphate. However, because these selectivity coefficients were derived from association constants calculated from titration experiments using only one anion, we performed the microarray experiments aimed at sensing of acetate in the presence of dihydrogenphosphate (H2P) (Figure 14, assay A) and chloride (Cl) (Figure 14, assay B), respectively. Both assays confirmed that, indeed, acetate may be sensed in water and in the presence of competing anionic substrates. From Figure 14 it is clear that changes in color start to be observable at an equimolar concentration of the target analyte/competitor (assay A: column 2 vs column 1) and (assay B: column 7 vs column 6). Further increase in the analyte (AcO) compared to the competitor concentration (assay A: column 2−5), (assay B: column 7−10) shows a gradual increase in the color change confirming that the change in color is due to the presence of the acetate analyte. This result is also significant

(67) (a) Schena, M. *Microarray Analysis*; Willey-Liss: Hoboken, NJ, 2003. (b) Vlasov, Y.; Legin, A.; Rudnitskaya, A.; Di Natale, C.; D'Amico, A. *Pure Appl. Chem.* **2005**, *77*, 1965−1983.
(68) Lavigne, J. J.; Anslyn, E. V. *Angew. Chem., Int. Ed.* **2001**, *40*, 3118−3130.

for potential application of anion sensing in biological media, where chloride and/or phosphate are often present. For example, human blood plasma contains 2 mM phosphate ($HPO_4^{2-}$) and 6 mM carboxylic acids/carboxylates.[69]

## Conclusion

Six years after being first described,[52] N-confused octamethyl calix[4]pyrrole was prepared on a multigram scale and unambiguously characterized by X-ray crystallography. As expected, the inverted pyrrole of NC-OMCP reacts preferentially at the unsubstituted α-position in electrophilic aromatic substitutions. Most importantly, the anion binding studies using N-confused calix[4]pyrroles revealed different anion selectivity compared to calix[4]pyrrole. Detailed NMR studies indicated that this rather unusual feature stems from a different binding mode, in which the anion is bound via three regular pyrrole NHs and appears to be in close contact with the *β*-CH of the inverted pyrrole in a conelike conformation. The materials utilizing the N-confused calix[4]pyrrole receptor exhibit a different binding preference compared to the parent octamethylcalix[4]pyrrole receptors. Thus a small difference in structure induces significant changes in supramolecular behavior. Finally, two pairs of chromogenic calix[4]pyrrole isomers were synthesized and characterized including X-ray crystallography. The anion binding assays revealed an interesting response of these potential anion sensors to various anions and was shown to follow the binding behavior observed for the respective parent receptors. Thus, regular OMCP-based materials show the anion affinity order $F^- > HP_2O_7^{3-} > AcO^- > H_2PO_4^- > Cl^-$, while the materials based on NC-OMCP show the following order of affinities: $AcO^- > F^- > HP_2O_7^{3-} > H_2PO_4^- > Cl^-$. This change in the affinity order is understood in terms of symmetry of the receptor and the receptor−anion complex, while the difference in color responses between OMCP and NC-OMCP derivatives is attributed to different distributions and energies of the frontier molecular orbitals responsible for the intramolecular partial charge transfer between the resting state and the anion complex. The different affinities and color responses between OMCP- and NC-OMCP-based sensors can be harnessed in anion sensing applications. Model colorimetric microassays were presented to sense selected anions administered in the form of their purely aqueous solutions while providing a clearly distinguishable change in color as a signaling output. Preliminary competitive assays suggest that these microassays may potentially be useful as anion sensors for carboxylates. Activities toward application of the above sensors for carboxylate sensing in biological milieu are currently under way in our laboratory.

**Acknowledgment.** P.A. gratefully acknowledges support from the Alfred P. Sloan Foundation, BGSU (Technology Innovations Enhancement grant), Kraft Foods, Inc., and the NSF (NER No. 0304320, SENSOR No. 0330267)

**Supporting Information Available:** X-ray crystallographic data (CIF files), $^1H$ NMR and absorption spectroscopic titration data for anion binding study (PDF). This material is available free of charge via the Internet at http://pubs.acs.org.

JA0622150

(69) Schmidt, R. F.; Thews, G. *Human Physiology*, 2nd ed.; Springer-Verlag: Berlin, 1989.